

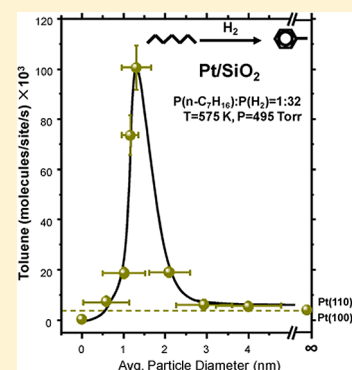
The Structure–Sensitivity of *n*-Heptane Dehydrocyclization on Pt/SiO₂ Model Catalysts

Matthew J. Lundwall,[†] Sean M. McClure,[†] Xin Wang,^{†,‡} Zhou-jun Wang,[†] Ming-shu Chen,^{†,‡} and D.Wayne Goodman^{*,†}

[†]Department of Chemistry, Texas A&M University, P.O. Box 30012, College Station, Texas 77842-3012, United States

[‡]State Key Laboratory of Physical Chemistry for Solid Surfaces, Department of Chemistry, College of Chemistry and Chemical Engineering, Xiamen University, Xiamen 361005, Fujian, China

ABSTRACT: The structure sensitivity of *n*-heptane dehydrocyclization has been evaluated on Pt nanoparticles as a function of Pt particle size. Pt particles were vapor-deposited onto a SiO₂ surface in ultrahigh vacuum (UHV) and then run under near-atmospheric pressures (495 Torr) by transferring the samples in situ to a batch reactor connected to the UHV system. The results demonstrate that the reaction rate increases as the particle size is decreased from 4 to 1.5 nm, consistent with results on high surface area technical catalysts. However, as particle size is further decreased below 1.5 nm, the reaction rate decreases, thus providing evidence of an optimum particle size for the dehydrocyclization reaction under the experimental conditions. The reactions on the nanoparticles are also compared with results obtained on Pt(100) and Pt(110) single crystals, which were run in the same apparatus under identical conditions. The differences between supported and unsupported Pt demonstrate that nanoparticles deactivate at a slower rate than single crystals, which suggests participation from the underlying silica support.



INTRODUCTION

Heterogeneous platinum catalysts often produce reaction products whose rates are dependent on the structure of the underlying platinum surface (i.e., structure sensitivity). One particular catalytic process that demonstrates this dependence is the conversion of hydrocarbons by platinum into aromatic, cyclic, lighter paraffins or olefins (or both).¹ For example, *n*-heptane can undergo a dehydrocyclization reaction to form toluene in addition to hydrogenolysis products.^{2,3} Formation of aromatics are of particular interest to both industrial and academic communities since they play an important role in petroleum refining and chemical processes. Defining which sites are more active in forming aromatics over cracked products can ultimately help in the design of new catalyst materials. However, the active sites that participate in such mechanisms are not well understood.

Fundamental studies on Pt single crystals have demonstrated dehydrocyclization to be a structure-sensitive reaction.^{2,3} The Pt(111) crystal plane is shown to be less active for dehydrocyclization by a factor of 2 than high-index Pt(557) surfaces, which contain six-atom-wide terraces (i.e., C₆) with one-atom-high steps (i.e., C₇ atoms).^{2–4} Interestingly, Pt-(10,8,7), which has a similar terrace/step combination to Pt(557) but is also covered by 6% kink sites (i.e., ≤ C₆), is shown to be slightly more active in forming toluene.³ However, highly corrugated surfaces such as Pt(25,10,7), which exhibits 9% kink sites and two-atom-wide terraces, is shown to have a lower reactivity than Pt(557) and Pt(10,8,7). These results suggest the size of the terrace to be an important parameter for *n*-heptane dehydrocyclization.

In a recent paper, we were able to quantify experimentally the percentage of various adsorption sites on the surface of Pt nanoparticles grown on silica in an ultrahigh-vacuum environment.^{5,6} The results have demonstrated that particles in the range of 4 nm exhibit similar concentrations of terrace sites, as observed on high-index single crystals. As the particle size is decreased below 4 nm, the percentage of terrace sites decreases dramatically. The structure of high-index, single-crystal surfaces cannot mimic the terrace/step site ratio of these highly dispersed particles. Carefully prepared and characterized model catalyst surfaces, consisting of Pt nanoparticles prepared on an oxide thin film support, present an opportunity to explore reactivity on highly stepped Pt nanoparticle surfaces and the role of support in the reaction.

Here, we assess *n*-heptane dehydrocyclization on well characterized Pt nanoparticles and relate the reaction rate to the concentration of available sites on these surfaces as a function of particle size. We employ reaction conditions similar to those that were conducted on the high-index crystals³ so that comparisons can be made when evaluating the structure–function relationship of Pt-catalyzed dehydrocyclization.

EXPERIMENTAL SECTION

The preparation and characterization of Pt/SiO₂ model catalysts have been described in detail in a previous publication.^{5,6} Briefly, silica films are grown in ultrahigh

Received: February 23, 2012

Revised: July 3, 2012

Published: July 16, 2012

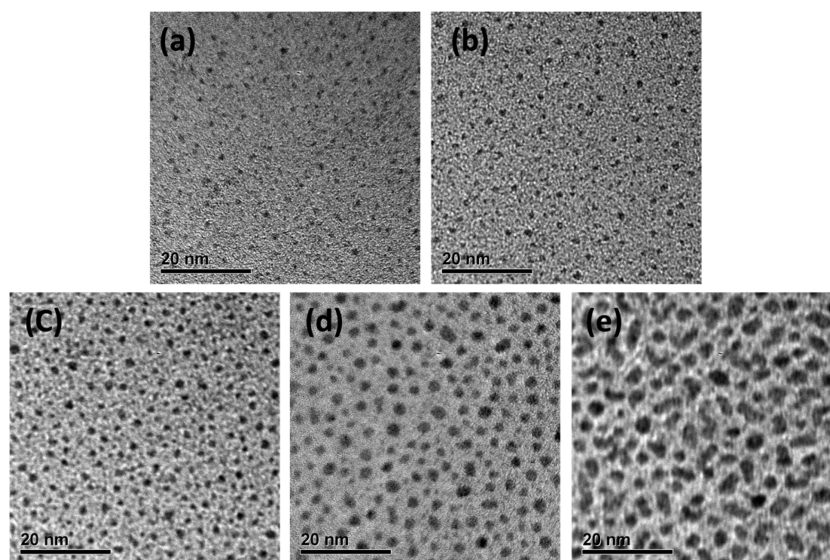


Figure 1. TEM images of Pt nanoparticles deposited on SiO₂: (a) 0.25 ML, (b) 0.50 ML, (c) 1 ML, (d) 2.0 ML, and (e) 6 ML. Images were taken using a JEOL JEM2010 at 200 keV. The SiO₂ film was grown on a carbon coated molybdenum grid in ultrahigh vacuum (UHV). SiO₂ film thickness is estimated to be 1.5 nm. Pt was also deposited in UHV and total deposited atoms are listed in monolayers (1 ML = 1×10^{15} atoms/cm²), as indicated.

vacuum (UHV) on both the front and rear side of a Mo(112) single crystal substrate (circular disk, 0.986 cm diameter) by vapor-depositing Si atoms in a 1×10^{-6} Torr oxygen environment at a sample temperature of 650 K. Temperature control and monitoring was established through resistive heating and a C-type thermocouple spot-welded to the crystal. Next, samples were annealed in 1×10^{-5} Torr oxygen at 1000 K to obtain an oxidized silica film. SiO₂ film thickness (1.5 nm) was obtained by observing complete attenuation of the Mo(112) (187 eV) MNN Auger transition.⁷ Silica films prepared in this manner exhibit vibrational modes comparable to vitreous bulk silica.⁸ Pt was subsequently vapor-deposited onto the silica film at ≈ 295 K, and total coverage of surface atoms was assessed by prior calibration of the Pt deposition rate through Auger electron spectroscopy (AES) on clean Mo(112).

Particle size estimates were obtained by comparison of CO chemisorption, hard-sphere calculations, and STM measurements.^{5,6} Particle size estimates were also obtained (in this study) using transmission electron microscopy (TEM). The samples for TEM were prepared on a carbon-coated molybdenum grid by vapor-depositing Si in an oxygen environment, followed by Pt under conditions identical to those on Mo(112). TEM measurements were performed ex situ with a JEOL JEM2010 at 200 keV. The average particle sizes from TEM were determined using the diameter-weighted average for >100 particles. Pt(110) and Pt(100) were also used for reactivity measurements. The temperature of Pt(110) and Pt(100) were monitored by a C-type thermocouple spot-welded to the sample. Each surface was cleaned prior to reaction by repeated oxygen annealing cycles in 5×10^{-7} Torr O₂ at 750 K, followed by final annealing at 1250 K in UHV. Surface cleanliness was monitored by AES until contamination (e.g., C, S) was below the AES detection limit.

Reactivity measurements were conducted in situ by translating the sample to a batch reactor coupled to the UHV surface analysis chamber.^{6,9,10} *n*-Heptane (Honeywell B&J brand >99.99% C₇, 99.38% *n*-heptane) was obtained and outgassed by multiple freeze, pump, and thaw cycles, followed by a triple

distillation prior to use. UHP hydrogen was used without further purification. Reactions were performed at a total pressure of $P_T = 495$ Torr at a ratio of 32:1 H₂/*n*-C₇H₁₆ and a temperature of 575 K to allow comparison with literature data.³ *n*-Heptane was administered into the reactor, followed by hydrogen. Rate measurements were obtained using gas chromatography (HP 5890, FID). Background reactions on the SiO₂/Mo(112) surface did not reveal any dehydrocyclization, hydrogenolysis, isomerization, or cyclization products over the course of our reaction time ($t = 1$ h). This indicates all reaction products are catalyzed from Pt nanoparticles. Reactions were kept at low conversions, typically <0.01%.

RESULTS AND DISCUSSION

Particle Size. Images for TEM experiments are shown in Figure 1. The images are presented at the same magnification so that direct comparisons can be made. Each Pt/SiO₂ TEM sample was prepared on a carbon-coated molybdenum grid. The SiO₂ films are estimated to be 1.5 nm thick (via AES) as determined by the silica deposition rate on the tantalum sample holder. Similarly as with SiO₂ deposition on Mo(112), the carbon-coating and Mo AES signals from the TEM grid were completely attenuated prior to Pt deposition at 298 K (i.e., all Pt particles grow on the SiO₂ overlayer). Vapor deposition of Pt atoms onto the silica-coated TEM grid exhibit the expected Volmer–Weber^{11,12} growth mode for Pt deposited on an oxide support, as evidenced by the formation of nanoparticles. It can be seen that the particles grow hemispherically and are monodisperse for low Pt coverages consistent with Pt deposited on silica thin films.^{5,6} The monodisperse characteristic and hemispherical nature of the Pt particles is lost as the Pt coverage increases above 2 ML, as shown by the images in Figure 1 and the size distributions of Figure 2. Figure 2 also displays the particle size dependence as a function of Pt monolayer coverage. It is observed that the particle size increases for increasing coverage along with a decrease in surface density (Figure 1), as expected for an Ostwald ripening mechanism and also consistent with Pt deposition on silica thin

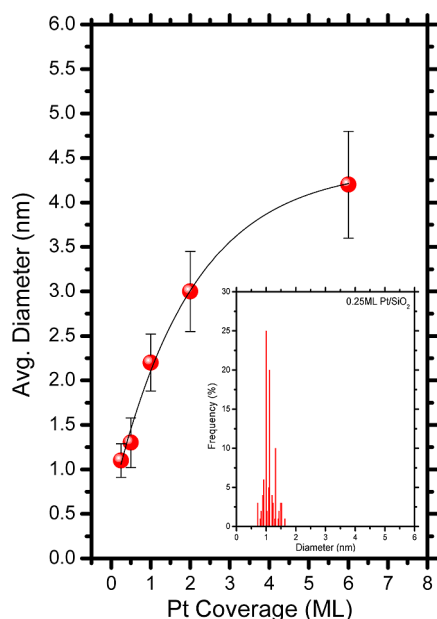


Figure 2. Particle size distributions obtained from TEM images of Figure 1. Inset is a histogram for 0.25 ML.

films.^{5,6,13} The errors in the particle sizes increase with increasing Pt coverage, since larger particles begin to grow amorphously. This effect is also observed in STM for Pt grown on ultrathin (1 ML) SiO₂ films.⁶ Particle size shown with TEM correlates well with particle size measured by CO TDS, modeling, and STM on SiO₂/Mo(112) for the Pt coverages listed (see below). Overall, these results correlate well with microscopy measurements conducted on bulk catalyst samples, which demonstrates that Pt nanoparticles grow hemispherically on silica.

Concentration of Step Sites. CO thermal desorption spectroscopy (TDS) measurements on Pt nanoparticles have been discussed in detail in a previous publication.⁵ The results allow a quantitative assessment of the site concentration on the surface of the Pt nanoparticles. Briefly, the desorption of CO from various Pt nanoparticle sizes gives rise to two desorption features, which can be assigned to “terrace-like” and “step-like” desorption sites. These sites on the nanoparticle are assigned as ≥ 8 fold coordination (e.g., C₉, C₈) or ≤ 7 fold coordination (e.g., C₇, C₆), respectively. We note that kink sites (i.e., $\leq C_6$) are also included in the assignment of “step-like” surface atoms.

Figure 3 demonstrates the concentration of step-like atoms on the surface of Pt nanoparticles obtained from the integrated area of the CO TDS measurements. Also presented in Figure 3 are hard sphere model calculations^{4,5} assuming nanoparticles grow in various geometric orientations: octahedrons, cuboctahedrons, rhombic dodecahedrons, and truncated cuboctahedron cap. It is clearly demonstrated that the site estimates from the CO TDS (under vacuum conditions) correlate well with the model describing nanoparticles as a hemispherically shaped cuboctahedron. The excellent overlap of CO TDS data with statistical calculations provides confidence when determining the concentration of step-like sites on small particles (<2 nm) (i.e., particles that could not be evaluated by the CO TDS methods). As such, when individual coordinations (i.e., C₇, C₆) are plotted with respect to particle size, as in Figure 4, it is shown that the percentage of C₆ kink sites approaches a maximum at ~ 1.5 nm. The C₇ trend becomes discontinuous

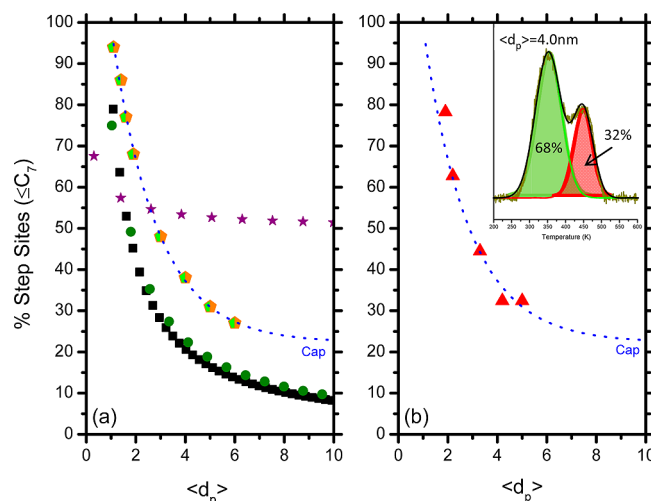


Figure 3. Concentration of step sites with coordination $\leq C_7$ as a function of average particle size $\langle d_p \rangle$, assuming various nanoparticle geometries.⁴ Graph a: octahedral (square), cuboctahedron (circle), rhombic dodecahedron (star), truncated cuboctahedron cap (hexagon). Graph b: the concentration of step sites obtained from thermal desorption spectroscopy⁵ of CO on Pt nanoparticles (triangle) plotted with the trend from the cuboctahedron cap. Inset in graph b is CO desorption data from $\langle d_p \rangle = 4$ nm.⁵

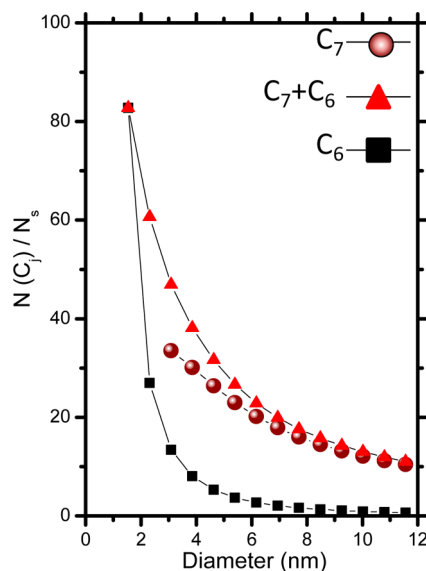


Figure 4. Concentrations of sites with coordination of C₇, C₆, and C₇ + C₆ on cuboctahedron.⁴

since particles in the size regime of 1.5 nm cannot support such sites. It is important to note that calculations^{1,5} show C₉ and C₈ terrace-like sites decrease dramatically with decreasing particles size. Moreover, it is also shown that small (i.e., <2 nm) particles do not exhibit terrace-like desorption features.⁵ The excellent comparison between the concentration of coordinated atoms from experimental and hard sphere models allows the characterization of Pt/SiO₂ model catalysts to approach the level of characterization demonstrated for metal single crystals. As such, the data allow a valuable and reliable reference point when evaluating reaction rates as a function of particle size.

Dehydrocyclization. Numerous catalytic studies have been conducted on the conversion of hydrocarbons by supported and unsupported Pt.^{1–3,14–19} It is understood that hydro-

genation reactions occur at lower temperatures and dehydrogenation, at higher temperatures. Both hydro/dehydro reactions require hydrogen in the reaction mixture to participate as a reactant or to reduce the potential for carbonaceous buildup on the surface. Rioux et al. have demonstrated hydrogenation to be dependent on the coverage of surface hydrogen.¹⁹ Smaller Pt particles are shown to be less active under high temperature or low hydrogen partial pressures (i.e., hydrogenation can exhibit structure-sensitive behavior). At lower temperatures or higher hydrogen partial pressure, hydrogenation exhibits structure-insensitive behavior. Dehydrogenation is generally considered to be structure-sensitive under various reaction conditions.¹⁹ It has been shown that as the Pt nanoparticle size is reduced, the dehydrogenation activity increases,¹⁹ which is consistent with studies of dehydrogenation on Pt(111) and Pt(557) single crystals.^{2,3}

The *n*-heptane dehydrocyclization mechanism is believed to occur through C6 ring closure, followed by dehydrogenation.¹ Gillespie et al.³ have demonstrated the *n*-heptane dehydrocyclization reaction to be favored on a surface that contains a combination of both terrace (e.g., C₉, C₈ coordination) and step (e.g., C₇, C₆ coordination) sites. The reaction rates on these stepped surfaces are shown to be more active by a factor of 2 than those on flat surfaces with close packed hexagonal structures (i.e., Pt(111)). Moreover, the rate has been shown to depend on terrace width. This is consistent with reactions of *n*-hexene on platinum, where terrace sites are important for aromatization.¹⁷ These results suggest the reactive ensemble at the surface must involve terrace atoms or a terrace step combination.

Figure 5 demonstrates the dehydrocyclization of *n*-heptane to toluene on Pt/SiO₂ and single crystal model catalysts expressed as a turnover frequency (TOF in molecules per site per second). The data are the initial rates of toluene formation

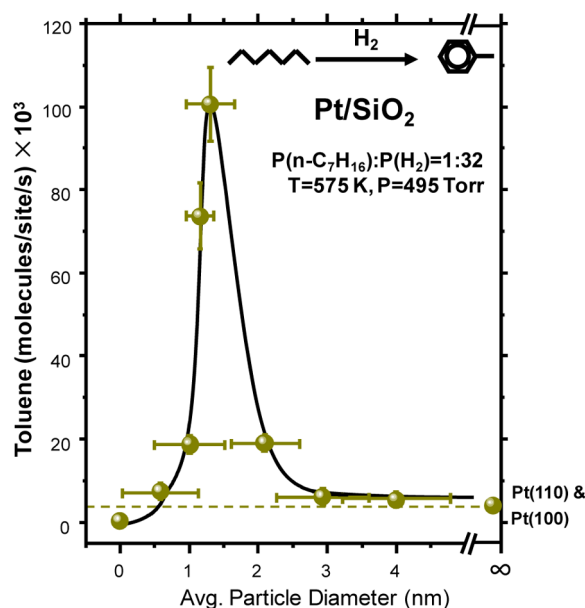


Figure 5. Dehydrocyclization of *n*-heptane expressed in molecules/site/s as a function of Pt particle size. Error bars represent standard deviation of repeated measurements on freshly prepared surfaces. Rate measurements on Pt(110) and Pt(100) obtained in the same apparatus exhibit similar rates. Both indicated by a dashed line (---).

at a conversion of <0.01%. Error bars represent the standard deviation of repeated measurements on freshly prepared surfaces. Pt(110) and Pt(100) were subjected to reaction conditions identical to those of the nanoparticles for accurate comparison. Both single crystal surfaces convert *n*-heptane to toluene with similar activity indicating C₈ (Pt(100)) and C₇ (Pt(110)) atoms to be active sites. The data in Figure 5 show almost an order of magnitude increase in the toluene rate as the average particle size is reduced from 4 to 1.5 nm. This trend in reactivity is comparable to the trend in the concentration of step sites on the surface as determined from CO TDS and hard sphere models (see Figure 3).⁵ What can be gleaned from this data is that larger (i.e., 4 nm) Pt nanoparticles behave similarly to single crystals, and step-like atoms are more favorable for dehydrocyclization than terrace-like sites. From the hard sphere model calculations and TDS measurements obtained from our previous publication,⁵ it can be determined that Pt particles with a size of 1.5 nm have a majority (80%) of their sites 6-fold coordinated C₆ (see Figure 4). When the size is decreased below 1.5 nm, the nanoparticles exhibit coordinations <C₆. Thus, the maximum in toluene formation rate occurs for Pt nanoparticles with the highest concentration of C₆ surface sites.

Interestingly, as the particle size is decreased below 1.5 nm (see Figure 5), the toluene formation rate begins to decrease. We can speculate several possible scenarios to explain this behavior. It could be that the silica substrate plays an unfavorable role in the reaction mechanism as particles size decreases below 1.5 nm. Certain oxides (e.g., TiO₂) are known to exhibit a strong metal support interaction.²⁰ If a similar phenomenon is occurring, the poor activity may arise from an electronic perturbation of the particles by the substrate or capping of the particles by silica; however, to our knowledge, this effect has not been reported for Pt/SiO₂, neither can we determine whether a similar process occurs *during* dehydrocyclization. Similarly, the loss of bulk properties (e.g., d-band filling) may affect the formation of key intermediates. Another possibility for the poor activity is that structures below 1.5 nm cannot support the appropriate reactive ensemble for dehydrocyclization or the heat of adsorption of hydrogen on various sites affects reactive pathways.¹⁹ Previous investigations have suggested the mechanism likely involves several adjacent atoms for binding of reactants.¹

To further explore the role of SiO₂ support in reactivity/deactivation, it is necessary to compare single crystals and particles of similar structure. When comparing the structures of Pt(110) and 5 nm particles, the concentration of C₇ atoms on Pt(110) is approximately equal to the 5 nm particle for a reconstructed Pt(110) surface and ~25% higher for an unreconstructed surface (see Figure 4). From the reactivity data, 5 nm nanoparticles and Pt(110) have similar reactivity after 1 h of reaction time (see Figure 5). Time-dependent data in Figure 6 shows the rate for 5 nm and Pt(110) rolls over (i.e., a continuous decrease in activity) as the reaction time is increased. The rate of this rollover is much slower for the 5 nm particles. Similarly to single crystals, the particles exhibited irreversible carbon deposits (i.e., carbon that cannot be removed by heating the surface in vacuum or in hydrogen³), as evidenced by AES (not shown). The carbon could be removed only by heating the surface in oxygen. It would then seem likely that the rollover on both systems is due to carbon buildup and that sites are blocked at a much slower rate on nanoparticles. Since the initial rate measurements demonstrate similar TOF for *clean* Pt nanoparticles and Pt(110), the

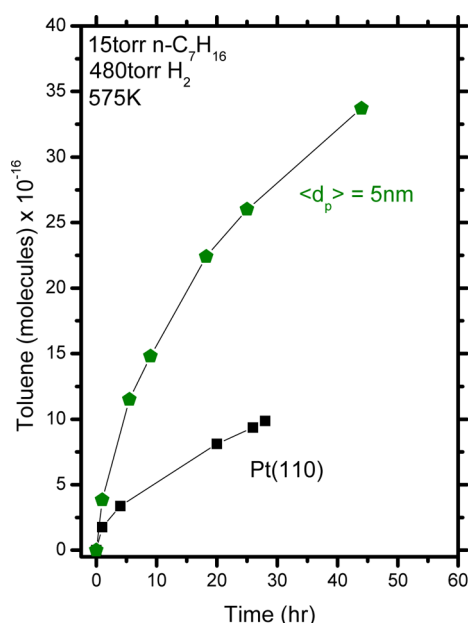


Figure 6. Time-dependent data for *n*-heptane dehydrocyclization on Pt/SiO₂ and Pt(110).

sustained reactivity of the Pt/SiO₂ model catalyst may be attributable to the silica support. This phenomenon may involve spillover of carbon atoms from the particle onto silica. Ongoing investigations in our laboratory are aimed at understanding the role of silica in model catalyst reaction studies.

CONCLUSIONS

This study offers a bridge between supported and unsupported Pt and provides insight into the structure–function relationship for *n*-heptane dehydrocyclization on Pt.^{1,3} The trend in toluene formation rate is shown to closely resemble the trend in under-coordinated atoms as the particle size is decreased to 1.5 nm. As such, the results have related the concentration of step sites at the nanoparticle surface to a change in catalytic activity. Moreover, the reaction exhibits a maximum in the formation rate of toluene at a particle size of ~1.5 nm, consistent with a reaction that would require 6-fold coordinated sites. As the Pt particle size decreases below 1.5 nm, the reaction rate exhibits a strong attenuation, which is most likely due to a loss of geometric and electronic effects required for dehydrocyclization. Time-dependent data indicate nanoparticles sustain their activity while the unsupported single crystalline platinum deactivates over the same period of time. Carbon formation on both the nanoparticle and single crystal surface is believed to be responsible for the loss in activity for both systems. Possibly, the underlying silica support plays a role in helping the nanoparticle sustain its reactivity.

AUTHOR INFORMATION

Corresponding Author

*Phone: +1 979 845 0214. Fax: +1 979 845 6822. E-mail: goodman@mail.chem.tamu.edu.

Notes

The authors declare no competing financial interest.

ACKNOWLEDGMENTS

We gratefully acknowledge support of this work by the Department of Energy, Office of Basic Energy Sciences, Division of Chemical Sciences, Geosciences, and Biosciences (DE-FG02-95ER-14511) and the Robert A. Welch Foundation (A-300). We thank the Microscopy and Imaging Center at Texas A&M University for access to the TEM.

REFERENCES

- (1) Davis, B. H. *Catal. Today* **1999**, 53, 443–516.
- (2) Joyner, R. W.; Lang, B.; Somorjai, G. A. *J. Catal.* **1972**, 27, 405.
- (3) Gillespie, W. D.; Herz, R. K.; Petersen, E. E.; Somorjai, G. A. *J. Catal.* **1981**, 70, 147–159.
- (4) Van Hardeveld, R.; Hartog, F. *Surf. Sci.* **1969**, 15, 189–230.
- (5) Lundwall, M. J.; McClure, S. M.; Goodman, D. W. *J. Phys. Chem. C* **2010**, 114, 7904–7912.
- (6) McClure, S. M.; Lundwall, M.; Zhou, Z.; Fang, F.; Goodman, D. W. *Catal. Lett.* **2009**, 133, 298–306.
- (7) Chen, M. S.; Santra, A. K.; Goodman, D. W. *Phys. Rev. B* **2004**, 69, 155404–1.
- (8) Wendt, S.; Ozensoy, E.; Wei, T.; Frerichs, M.; Cai, Y.; Chen, M. S.; Goodman, D. W. *Phys. Rev. B* **2005**, 72, 115409.
- (9) McClure, S. M.; Lundwall, M. J.; Goodman, D. W. *Proc. Natl. Acad. Sci. U.S.A.* **2011**, DOI: 1006635107v1-6.
- (10) McClure, S. M.; Lundwall, M.; Yang, F.; Zhou, Z.; Goodman, D. W. *J. Phys. Chem. C* **2009**, 113, 9688–9697.
- (11) Venables, J. A. *Surf. Sci.* **1994**, 299/300, 798–817.
- (12) Usher, B. F. *App. Sur. Sci.* **1985**, 22/23, 506–511.
- (13) Ramachandran, A. S.; Anderson, S. L.; Dayte, A. K. *Ultramicroscopy* **1993**, 51, 282–297.
- (14) Davis, S. M.; Somorjai, G. A. *J. Catal.* **1980**, 65, 78.
- (15) Davis, S. M.; Zaera, F.; Somorjai, G. A. *J. Catal.* **1984**, 85, 206–223.
- (16) Zaera, F.; Godbey, D.; Somorjai, G. A. *J. Catal.* **1986**, 101, 73–80.
- (17) McCrea, K. R.; Somorjai, G. A. *J. Mol. Catal., A: Chem.* **2000**, 163, 43.
- (18) Wilson, J.; Guo, H.; Morales, R.; Podgornov, E.; Lee, I.; Zaera, F. *Phys. Chem. Chem. Phys.* **2007**, 9, 3830–3852.
- (19) Rioux, R. M.; Hsu, B. B.; Grass, M. E.; Song, H.; Somorjai, G. A. *Catal. Lett.* **2008**, 126, 10–19.
- (20) Tauster, S. J. *Acc. Chem. Res.* **1987**, 20, 389–394.